JOURNAL OF APPLIED ELECTROCHEMISTRY 18 (1988) 268–279

Passive films on magnesium anodes in primary batteries

B. V. RATNAKUMAR

Jet Propulsion Laboratory, California Institute of Technology, 4800 Oak Grove Drive, Pasadena, CA 91109, USA

Received 10 July 1987; revised 21 September 1987

The characteristics of the passive films over Mg anodes, which essentially govern the voltage delay of the latter, have been determined non-destructively from an analysis of the transient and steady-state response of the electrode potential to low-amplitude galvanostatic polarization under various experimental conditions *viz.*, with different corrosion inhibitor coatings on Mg, after various periods of ageing of anode in solutions containing corrosion inhibitors, at various low temperatures etc. Using these parameters, the kinetics of film build-up or dissolution under these conditions have been monitored. The morphology of the anode film has been predicted from a combination of potential-time transients at low c.d.s and delay-time curves during ageing and verified with scanning electron microscopy. Similar transients at low temperatures point out a steep rise in the film resistivity which is essentially responsible for the severe voltage delay. Finally, possible application of this technique in secondary Li batteries to improve cycling characteristics of the Li anode has been pointed out.

1. Introduction

Magnesium batteries offer several advantages over the conventional zinc-based systems namely, high cell voltage high energy densities per unit weight and volume especially at high power densities and low discharge temperatures and a long shelf life at ambient as well as high storage temperatures. The long storage life is possible owing to a protective film over Mg, which is also responsible for the voltage delay of magnesium batteries.

The voltage delay characteristics of the Mg anode are essentially governed by the breakdown kinetics of the passive film, i.e. by its resistance, capacitance, dielectric strength etc. [1, 2]. A measurement of these parameters could thus help to predict the voltage delay characteristics of the Mg anode. Also, it would throw light on the morphology of the passive film. A coherent barrier-type film, for instance, exhibits a high resistance of 10^3–$10^5\,\Omega\,cm^2$ whereas a porous film has resistance orders of magnitude lower. It is, therefore, of both theoretical as well as practical interest to determine the characteristics of the passive film over Mg.

In the present work, a relatively simple and non-destructive method involving measurement and interpretation of potential response to low-amplitude galvanostatic pulse is adopted for the determination of resistance and capacitance of the passive films over Mg in contact with the battery electrolyte $Mg(ClO_4)_2$ under various experimental conditions *viz.*, with different corrosion-inhibitor coatings on Mg, after different periods of ageing of the anode in solutions containing corrosion inhibitors, at various low temperatures etc.

1.1. *Earlier work*

Attempts made in the literature include (a) a.c. impedance method [3, 4] which requires sophisticated equipment and profound knowledge of the theory; (b) d.c. current-interruption method [5] wherein the anode film breaks down at the c.d.s applied; (c) potentiostatic pulse method [6, 7] which is inapplicable due to surge currents during switching-on and switching-off operations damaging the film, etc. Recently, Moshtev *et al.* developed a galvanostatic pulse method (GPM) for the passive films over Li [8–12], wherein the film capacitance is evaluated from high-amplitude short-duration pulse and the film resistance from low-amplitude long-duration pulse.

A more reliable method, essentially an improvement over GPM, has been employed by Sathyanarayana *et al.* [13] for the determination of anode-film resistance and double-layer capacitance in $Mg-MnO_2$ dry cells. Here, both the film resistance and film capacitance could be calculated from the potential response to a single low-amplitude long-duration pulse. This method termed as 'galvanostatic micropolarization' has been adopted in the present work. Owing to the insulating and dielectric properties of the film, the Mg-solution interface exhibits a noticeable potential transient even at low c.d.s, as shown by a typical transient in Fig. 1, similar to the charging/discharging processes of a resistor-capacitor combination. On terminating the polarization, the potential attains the original value in the same exponential manner, with no overshoot that follows film breakdown [14]. From the potential transient, the film resistance and film capacitance could be evaluated as shown below.

2. Mg-film solution interface

2.1. *Porous film*

In the case of a thick anode film containing flaws *viz.*, pores/fissures/cracks [2], the charge transfer involving

0021-891X/88 $03.00 + .12

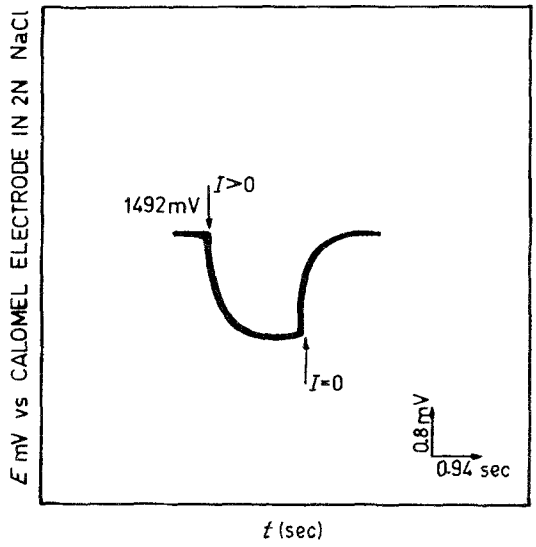

Fig. 1. A typical potential-time transient of a Mg anode in contact with 1 N $Mg(ClO_4)_2$ solution saturated with $Mg(OH)_2$ (pH: 8.5) and containing 0.3 g l^{-1} of Li_2CrO_4 during initiation ($I > 0$) and termination ($I = 0$) of galvanostatic micropolarization (40 nA cm^{-2}).

the ionization of Mg is localized at the metal-film interface, essentially at the sites where the base metal is exposed directly to the electrolyte seeped through the flaws. The equivalent circuit would thus be a parallel arrangement of capacitances due to film-covered and film-free portions in series with a parallel combination of resistances due to film-covered and film-free areas with the electrolyte resistance (see Fig. 4 in [2]). Accordingly, the interfacial resistance and capacitance are essentially governed by those of film-free areas. The interfacial resistance thus being low, the metal-porous film-solution interface would not exhibit any potential transient at low anodic c.d., i.e. during micropolarization.

2.2. *Barrier film*

The Mg-barrier film-solution interface could be represented by an equivalent circuit consisting of interfacial capacitance parallel with the film resistance and the charge-transfer resistance, the electrolyte resistance being in series with the above combination [13]. Any instantaneous change in potential would thus correspond to electrolyte resistance which is negligibly small as compared to the film resistance.

At low anodic c.d.s (10–100 nA/cm^2) the interface exhibits a distinct potential transient due to the high resistance/low capacitance of anode film. Also, during micropolarization, the dilation stresses generated due to accumulation of reaction product at the interface and/or the thickening of the film would be insignificant (the amount of charge passed, 20 nA cm^{-2} for a maximum of 30 sec, i.e. 0.6 μC cm^{-2} corresponds to 0.3% of a monolayer of $Mg(OH)_2$, the reaction product (200 μC cm^{-2} = 1 monolayer of $Mg(OH)_2$ assuming an interatomic distance of 3 Å)) and the anode film is unaffected. At high anodic c.d.s, the interface exhibits voltage delay with a potential undershoot attributed to the film resistance and the potential recovery ascribed to film breakdown by ionic flux-induced dilatation effects [2]. The expression for the potential transient during galvanostatic micropolarization [13] is:

$$\eta = -(R_t + R_f)I + K[\exp - \{t/(R_t + R_f)C_f\}] \quad (1)$$

with $R_t = [I_{corr}(\alpha + \beta)f]^{-1}$.

Here C_f is the capacitance and R_f the resistance of the film covering the anode of overpotential η at any instant 't'; I_{corr} is the specific corrosion current, α and β the apparent energy transfer coefficients for cathodic and anodic partial reactions, K is the integration constant and $f = F/RT$.

2.2.1. Evaluation of integration constant. On differentiating the above equation:

$$\frac{d\eta}{dt} = \frac{-K}{(R_t + R_f)C_f}[\exp - \{t/(R_t + R_f)C_f\}] \quad (2)$$

which at $t \longrightarrow 0$ reduces to:

$$\left(\frac{d\eta}{dt}\right)_{t\to 0} \approx \frac{-K}{(R_t + R_f)C_f} \quad (3)$$

At $t \longrightarrow 0$, i.e. immediately after initiating the polarization, the net current I may be approximated to the charging current I_{ch}, i.e.

$$-C_f\left(\frac{d\eta}{dt}\right)_{t\to 0} = [I_{ch}]_{t\to 0} \approx I \quad (4)$$

From equations 3 and 4

$$K = (R_t + R_f)I \quad (5)$$

substitution of which into equation 1 gives the time dependence of electrode potential during galvanostatic micropolarization of Mg anode as

$$\eta = (R_t + R_f)I[\exp\{-t/(R_t + R_f)C_f\} - 1] \quad (6)$$

2.2.2. Calculation of film characteristics. Film resistance: The film resistance could be obtained from the steady-state overpotential η_∞ which according to equation (6) is

$$\eta_\infty = -(R_t + R_f)I \quad (7)$$

The value of R_f, the film resistance is orders of magnitude higher than R_t, the reaction resistance, as is evident from a total extinction of the potential transient immediately after the breakdown of the passive film at high c.d.s. The interfacial resistance at high (higher than film breakdown potential) anodic potentials which largely constitutes reaction resistance is 1–2 Ω cm^2 [6, 7] whereas at passive potentials the interfacial (film) resistance is 10^3–10^4 Ω cm^2.

The reaction resistance R_t may therefore be neglected in equation 7 and the film resistance may be calculated therefrom.

Film capacitance: from equation 6:

$$\ln\left(\frac{d\eta}{dt}\right) = \ln\left(\frac{-I}{C_f}\right) - \frac{t}{(R_t + R_f)C_f} \quad (8)$$

A plot of ln $(d\eta/dt)$ vs t should therefore be linear, the slope of which gives $(R_t + R_f)C_f$. With the value of $(R_t + R_f)$ calculated above, the film capacitance could be evaluated. Alternatively, the film capacitance could be calculated from the intercept ln $(-I/C_f)$ (the film capacitances over uncoated, chromate-passivated, olive oil-coated, coconut oil-coated and chromate-passivated coconut oil-coated Mg anodes in the electrolyte solution (without chromate) estimated from the slopes of ln $(d\eta/dt)$ vs t plots are 128.4, 76.6, 2.82, 2.0 and 5.4 μF cm^{-2} respectively and are of the same order as those obtained from intercepts *viz.*, 76.5, 40, 4.54, 2.3 and 4.77 μF cm^{-2} respectively) which, however, was not adopted in the present work.

2.2.3. Open-circuit transient. Since no additional information is derived from an analysis of the open-circuit recovery transient [13], the present study is confined to the potential transients during current injection only.

3. Experimental details

The experimental details on the pretreatment of the working electrode (AZ21 from DOW chemicals, USA), the electrolytic cell, the preparation of the electrolyte solution, the inhibitor coating over the working electrode were given in [1]. The electrolyte solution which is 1 N $Mg(ClO_4)_2$ saturated with $Mg(OH)_2$ (pH: 8.5) also contained 0.3 g l^{-1} of Li_2CrO_4 whenever inhibition of Mg corrosion was required.

Experiments were begun within one hour after the pretreatment of the WE and electrochemical measurements were carried out within 15 minutes after electrolyte filling during which an equilibrium in the electrode potential had set in.

Corrosion rates were measured from current-potential curves during steady-state galvanostatic cathodic polarization as in equation 1. The delay time curves, i.e. potential-time transients at high c.d. were also obtained in a similar fashion as in equation 1.

The electrical circuit (Fig. 2) employed for monitoring the potential transients during galvanostatic micropolarization is essentially the same as in [13] and consists of a polarization circuit, voltage back-off circuit and the recording equipment interfaced with an electrometer to avoid loading errors in the measured electrode potentials.

4. Results and discussion

4.1. *Uncoated Mg*

The potential-time transient during galvanostatic micropolarization (at 20 nA cm^{-2}) of uncoated Mg anode immediately after its immersion in the electrolyte solution is shown in Fig. 3. The salient features of the above transient are:

(a) The absence of any noticeable, instantaneous drop in potential, suggesting a negligible ohmic polarization across the solution.

(b) A slow exponential approach of the electrode potential to the steady-state value, implying a dielectric film.

(c) A significant steady-state overpotential even at low c.d.s, pointing out a high film resistance.

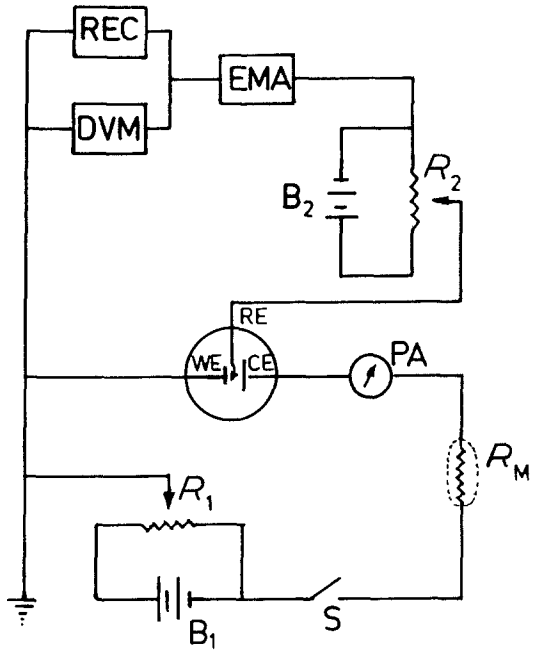

Fig. 2. Experimental set-up for non-destructive galvanostatic micropolarization of Mg anode (WE) against stainless steel counter electrodes (CE) with a calomel electrode in 2 N NaCl as the reference electrode (RE). (B1) Nickel cadmium battery of 12 V, 20 Ah (SAFT) at 50% state of charge; (B2) Nickel cadmium battery of 6 V, 12 Ah (SAFT) at 50% state of charge; (R_1 & R_2) Ten-turn, 10 KΩ helical potentiometers; (R_M) Shielded mega ohm (22 MΩ) resistance; (PA) Kiethley picoammeter; (EMA) Kiethley electrometric amplifier with input impedance > 10^{12} Ω and at unit gain; (REC) Rikadenki strip chart recorder with a maximum sensitivity of 0.4 mV cm^{-1} and chart speed of 2.13 cm sec^{-1}; (DVM) Digital voltmeter with a high input impedance; (S) Switch to initiate polarization.

4.1.1. Film resistance. The resistance of the passive film over uncoated Mg anode calculated from Fig. 3 is 15 kΩ cm^2. This is of the same order as in alkaline fluoride solutions [5]. Perrault [6, 7] referred to this as

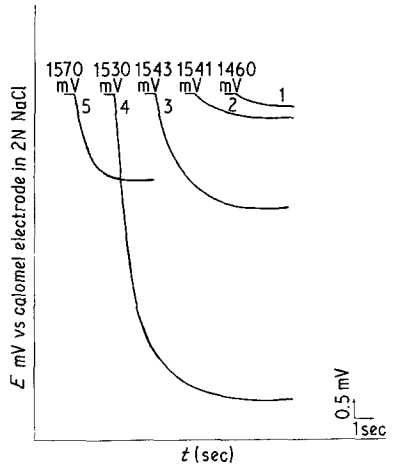

Fig. 3. Potential-time transients of (1) uncoated; (2) chromate-passivated; (3) olive oil-coated; (4) coconut oil-coated and (5) chromate-passivated and coconut oil-coated Mg anode (area: 5 cm^2) in contact with 1 N $Mg(ClO_4)_2$ solution saturated with $Mg(OH)_2$ (pH: 8.5) during initiation of galvanostatic micropolarization of 20 nA cm^{-2}.

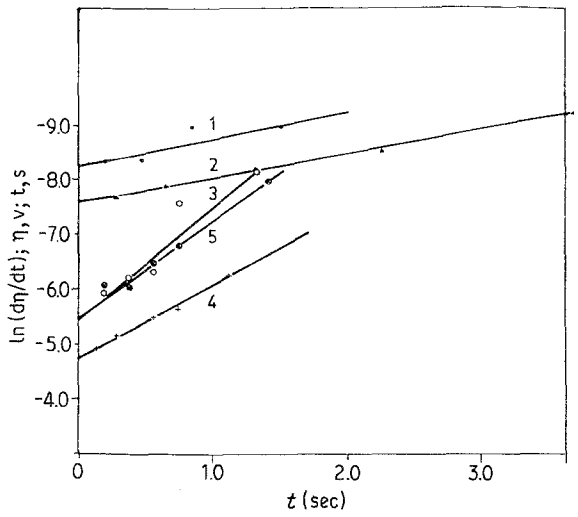

Fig. 4. Plots of ln ($d\eta/dt$) against t (equation 8 in the text) of (1) uncoated, (2) chromate-passivated, (3) olive oil-coated, (4) coconut oil-coated and (5) chromate-passivated and coconut oil-coated Mg anode recast from Fig. 3.

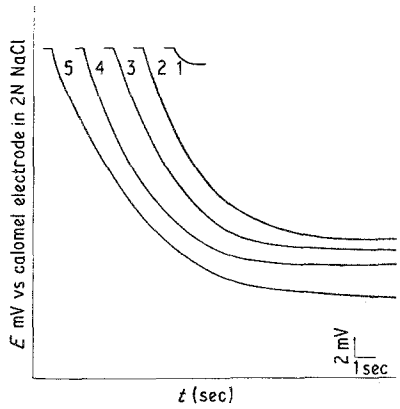

Fig. 5. Potential-time transients of uncoated Mg anode, during galvanostatic micropolarization of 40 nA cm^{-2}, after ageing for (1) 15 min; (2) 18 h; (3) 24 h; (4) 41 h; and (5) 74 h in 1 N $Mg(ClO_4)_2$ solution saturated with $Mg(OH)_2$ and containing 0.3 g l^{-1} of Li_2CrO_4.

an 'infinitely high resistance' around the open-circuit potential, as compared to the low interfacial resistance of 0.1–1.0 Ω cm^2 at high anodic potentials where film ceases to exist.

4.1.2. Film capacitance. The plot between t and ln ($d\eta/dt$) (equation 8) recast from Fig. 3 is linear (Fig. 4). The capacitance of uncoated Mg anode calculated from its slope and the film resistance is 128 μF cm^{-2}. Despite seeming to be high for a film covered electrode, the above value is (a) of the same order (i.e. 50 μF cm^{-2}) as in neutral $MgSO_4$ solutions obtained by a.c. impedance [3]; (b) consistent with Perrault's observation [6, 7] that the capacitance of Mg electrode in near-neutral solutions ranges from 2000 μF cm^{-2}–2 μF cm^{-2}, depending on the extent of passive film formation (in solutions without chromate inhibitor the corrision rate of Mg is very high, especially of uncoated Mg (Table 1) pointing to a rapid dissolution of the initial air-formed film) and (c) expected for an etched and thus rough electrode.

4.1.3. With chromate inhibitor. The potential-time transient of uncoated Mg anode is more pronounced in solution with chromate inhibitor than without (compare curves (1) of Fig. 3 and Fig. 5), with an increase in the steady-state overpotential as well as the time required to attain the same. The film resistance increases to 38 kΩ cm^2 and the film capacitance decreases to 48 μF cm^{-2}, as also observed earlier [3], which is due to a build-up, over the initial film, of corrosion products of Mg (essentially $Mg(OH)_2$ and $MgCrO_4$) during the stabilization time of 15 minutes after immersing the anode in solution. The flaws in the initial film would thus heal up and also the film would thicken. In solutions without chromate the corrosion products form a porous film as described below (Section 4.3).

4.2. *Passive films impregnated with corrosion inhibitors*

The potential-time transients during micropolarization of Mg anodes coated with various corrosion inhibitors such as $MgCrO_4$ (passivated by chromate-dip), esters of long-chain fatty acids (coconut oil and olive oil) and a combination of chromate and coconut oil, are larger than that of uncoated Mg (Fig. 3), owing to the resistive and dielectric properties of the inhibitor layer.

4.2.1. Film resistance. The film resistances evaluated from the transients in Fig. 3 are 30 kΩ cm^2 and 100–400 kΩ cm^2 for the chromate-passivated and oil-coated Mg respectively (Table 1). Among the coated Mg anodes, the film resistance increases as:

uncoated < chromate passivated ≪ oil-coated

which may be due to the thickness of the passive layer increasing in the above order (see Section 4.3.3., Table 1). Since the mechanism of corrosion inhibition by the above inhibitors is by 'ohmic control' [1], it is expected that the corrosion of Mg would decrease with an increase in the film resistance, i.e. in the above order. The corrosion rates estimated from steady-state galvanostatic cathodic polarization curves are in agreement with the above deduction (Table 1).

4.2.2. Film capacitance. The capacitances of chromate-passivated and oil-coated Mg anodes, evaluated from the slopes of ln ($d\eta/dt$) vs t plots (Fig. 4) are 76 μF cm^{-2} and 2–5 μF cm^{-2} respectively (Table 1). Again, the capacitance is reduced to half by chromate passivation and by about an order of magnitude with oil coating. Among the coated Mg anodes, the capacitance decreases as:

uncoated > chromate-passivated ≪ oil-coated

which may be attributed to the thickness of the anode film increasing in the above order (Section 4.3.3) and also the dielectric constants of the inhibitor decreasing as

Table 1. Characteristics of passive films over uncoated and coated magnesium anodes evaluated from potential-time transients during micropolarization under various experimental conditions

NATURE OF COATING ON Mg	DIELECTRIC CONSTANT OF FILM MATERIAL ϵ (LITERATURE)	RESISTIVITY OF FILM MATERIAL ρ ohm cm CALCULATED	IN $(Mg(ClO_4)_2$ pH 8.5						IN $Mg(ClO_4)_2$ (pH: 8.5) + 03 g/LIT Li_2CrO_4											
			CORR. RATE OF Mg $\mu A/cm^2$	AGEING TIME, h	AGEING STUDIES				CORROSION RATE OF Mg ($\mu A\,cm^{-2}$)	AGEING TIME, h	AGEING STUDIES					LOW TEMPERATURE				
					TRANSIENT PARAMETERS						TRANSIENT PARAMETERS					TEMP °C	TRANSIENT PARAMETERS			ACTIVATION ENERGY FOR CONDUCTION eV
					R_f $K\Omega cm^2$	$\frac{d\ln(d\eta/dt)}{dt}$	C_f $\mu F\,cm^{-2}$	FILM THICKNESS Å			R_f $K\Omega cm^2$	$\frac{d\ln(d\eta/dt)}{dt}$	C_f $\mu F\,cm^{-2}$	FILM THICKNESS Å	RATE CONSTANT FOR GROWTH cm^2/s		R_f $K\Omega cm^2$	$\frac{d\ln(d\eta/dt)}{dt}$	C_f $\mu F\,cm^{-2}$	
UNCOATED (Mg HYDROXIDE)	8.2	2.55×10^{12}	13.84	0	15	0.52	128.4	0.57	5.02	0	38	0.548	4.8	1.4	3.33×10^{-19}					
				18	–	–	–	–		18	463	0.415	5.2	17.4						
										24	485	0.644	3.2	18.3						
										41	525	0.651	2.9	19.8						
										72	563	0.639	2.7	21.2						
CHROMATE PASSIVATED (Mg CHROMATE)	8.2	3.17×10^{12}	5.51	0	30	0.435	76.6	0.95	4.18	0	52	0.534	36	1.6	0.434×10^{-19}	27	175	0.15	38	0.2065
				18	–	–	–	–		18	128	0.285	27.4	4.0		10	437	0.0425	34.8	
										24	130	0.298	25.8	4.1		0	1187	0.033	25.2	
										48	135	0.31	20	4.3		-10	1325	0.01825	41.4	
										72	140	0.42	17	4.4		-20	1615	0.0205	29.1	
																-27	2500	0.01	40.0	
OLIVE OIL	3.0	1.68×10^{12}	0.76	0	155	2.286	2.82	8.89	0.73	0	135	0.52	14.2	7.7						
				18	125	0.88	9.09	7.11		18	125	0.56	14.3	7.1						
				24	110	1.2	7.57	6.22		24	115	0.60	14.4	6.5						
				41	98	0.571	17.8	5.51		41	110	0.62	14.66	6.2						
				89	65	0.137	112	3.54		48	105	0.65	15.2	5.9						
COCONUT OIL	3.0	2.75×10^{12}	0.53	0	375	1.32	2.0	13.66	0.25	0	385	0.72	3.6	14.0						
				18	80	1.02	11.6	2.93		18	675	0.585	2.53	24.6						
				24	60	0.89	18.7	2.20		24	750	0.596	2.44	27.3						
				41	50	1.05	19.05	1.84		48	800	0.588	2.125	29.1						
				48	43	0.91	25.5	1.59		96	830	0.602	2.0	30.2						
				96	20	0.76	65.8	0.74												
CHROMATE PASSIVATION AND COCONUT OIL	–	–	0.76	0	100	1.85	5.4	3.43	0.32	0	210	0.74	6.16	7.2						
				18	30	1.45	23.0	1.03		18	270	0.74	5.02	9.2						
				24	15	1.69	41.7	0.51		24	875	0.54	2.11	29.9						
				41	12.5	1.09	73.4	0.43		41	980	0.505	2.02	33.6						
				48	10	0.83	120.5	0.34		65	1300	0.53	1.44	44.5						
				87	5	0.53	377.4	0.17		137	1310	0.541	1.41	44.9						

magnesium hydroxide ≈ magnesium chromate

> coconut oil or olive oil

It was deduced in [2] that lower the capacitance of the anode film, faster would be the initiation of its breakdown and hence, shorter would be the voltage delay. Accordingly, the lower capacity of oil-coated anodes explains their more rapid recovery of potential than in uncoated anode as observed earlier [1].

4.2.3. Solutions containing chromate. In the case of coated Mg anodes, the potential-time transients as well as the film characteristics evaluated therefrom are virtually the same in solutions with or without chromate. There is no such increase in the film resistance/decrease in the film capacitance on adding Li_2CrO_4 to the solution as observed with uncoated Mg anode (Table 1). This may be attributed to the corrosion rate of Mg which is responsible for a build-up of anode film, being reduced considerably by the inhibitor coating over Mg.

4.3. *Ageing of the anode in solution*

The voltage delay of Mg increases during its ageing in solution due to a growth of anode film by a deposition of corrosion products of Mg during ageing [1]. Accordingly, an increase in film resistance and reciprocal film capacitance are expected during ageing of Mg in solution, which would be verified below at different corrosion rates of Mg, i.e. in solutions with and without chromate inhibitor.

4.3.1. Solutions containing chromate. The potential-time transients during micropolarization of uncoated Mg after different periods of its ageing in solutions containing chromate (Fig. 5) demonstrate the expected increase in the transient behaviour on ageing. The transient parameters calculated therefrom, namely, film resistance and reciprocal film capacitance increase sharply in the initial stages and sluggishly in the later stages of ageing (Table 1), owing to a build-up of anode film. Also, it may be inferred from the above 'order of magnitude' increase in film resistance that the corrosion products deposit over the initial film as a coherent and barrier type layer; a porous layer would not exhibit any noticeable resistance measureable from potential transients during micropolarization. The delay-time curves of uncoated Mg after ageing in solution containing chromate (Fig. 6) exhibit an instantaneous potential drop attributed to ohmic polarization across the film, followed by a rapid recovery in potential. The ohmic drop increases during ageing due to build-up of barrier-type film and is mainly responsible for the elongation of voltage delay during ageing.

4.3.2. Coated Mg. It was observed earlier [1] that coatings of corrosion inhibitors, e.g. esters of long-chain fatty acids, over Mg, reduce the growth rate of the anode film and thus minimize the elongation of voltage delay during ageing. Accordingly, potential transients during micropolarization as well as the film resistance and reciprocal film capacitance calculated therefrom increase at a slower rate in the case of coated as compared to uncoated Mg (Table 1). This could be predicted from the corrosion rates of Mg decreasing with inhibitor coating (Table 1) as

uncoated > chromate-passivated

≫ oil-coated Mg anode.

With coconut oil coating, however, the film resistance as well as reciprocal capacitance increase rather sharply, which is not expected for the low corrosion rate of anode (Table 1). This could possibly be due to the formation of an additional resistive layer over Mg of a Mg salt of essentially lauric acid, similar to the saponification reaction of esters in alkaline solutions.

The rates of saponification are widely different between coconut oil and olive oil, the former undergoing the same at appreciable rates even at ambient temperatures, whereas the latter requires high temperatures and for a long time. Consequently, the above reaction with electrolyte would not occur as readily in the case of olive oil. On the other hand, a slight decrease in the film resistance over olive oil-coated Mg is observed during ageing, which may be due to a slow dissolution of olive oil in slightly alkaline solutions as in the present case.

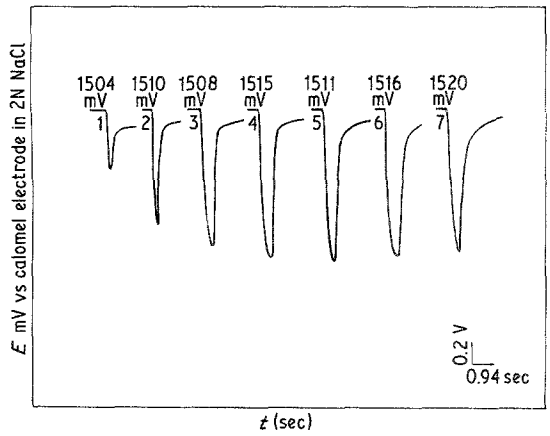

Fig. 6. Delay time curves of uncoated Mg anode, at a c.d. of 1 mA cm^{-2}, after ageing for (1) 15 min; (2) 16 h; (3) 23 h; (4) 47 h; (5) 54 h; (6) 95 h; and (7) 147 h; in 1 N $Mg(ClO_4)_2$ solution saturated with $Mg(OH)_2$ (pH: 8.5) and containing 0.3 g l^{-1} of Li_2CrO_4.

4.3.3. Film thickness. The thickness of anode film may be estimated from the film capacitance with the assumption of a parallel-plate capacitor model which is reasonable in concentrated solutions. Assuming a roughness factor of unity, the film thickness, L, may be estimated as

$$L = \frac{8.85 \times 10^{-8} \times \varepsilon}{C_f} \text{ cm} \qquad (9)$$

where C_f is expressed in μF cm^{-2} and ε is the dielectric constant of the film material.

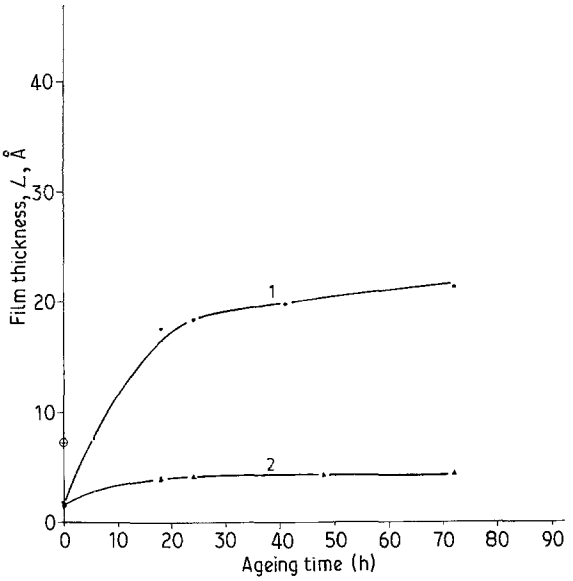

Fig. 7. Variation of film thickness over (1) uncoated and (2) chromate-passivated Mg anode during its ageing in 1 N $Mg(ClO_4)_2$ solution saturated with $Mg(OH)_2$ (pH: 8.5) and containing 0.3 $g\,l^{-1}$ of Li_2CrO_4.

The thicknesses of various films over Mg in solutions with and without chromate inhibitor are listed in Table 1.* While estimating the above, it was assumed that the inhibitor layer is superimposed on the initial passive film present over uncoated Mg and the effective resistance/capacitance is a resultant of both in series. The resistivities of various corrosion inhibitors evaluated from the resistance and thickness are listed in Table 1.

The thicknesses of passive films after different periods of ageing were estimated from the above resistivities as:

$$L = \frac{R_f}{\varrho}\ \text{cm} \tag{10}$$

where R_f is the film resistance in $\Omega\,cm^2$ and ϱ is the film resistivity in Ω cm (Table 1). (The film thicknesses calculated from either equation 9 or 10 are in close agreement.)

The growth of anode film during ageing is well demonstrated in Fig. 7. The growth rate is parabolic with an initial exponential increase followed by an asymptotic approach to the steady-state value; the latter being due to the fact that the thickening of anode film would inhibit the corrosion of Mg and thus reduce further film growth. Also, the growth rate is less in coated Mg for, e.g. chromate-passivated Mg, as compared to uncoated Mg, thus conforming to the 'corrosion-deposition-growth' model described in [1]. Coconut oil-coated anodes, however, exhibit a high rate of film growth, unexpected from their low corrosion rates, possibly due to the reaction of the outer layer of coconut oil with alkaline electrolyte, resulting in the formation of insulating layer of lauric acid-Mg salt as explained in Section 4.3.2.

4.3.4. Rate constant for film growth. The corrosion of Mg involves hydrogen evolution as the cathodic conjugate reaction, the open-circuit potential of Mg being a mixed value [1]. The anode surface contains either chemical or metallurgical heterogenities which result in the formation of local galvanic cells. The rate determining step for the corrosion would be diffusion/migration of cathode reactants since Mg compounds (such as oxides) are known to be anion conductors with a transport number, t_- close to unity [16].

The processes contributing to film growth *viz.*, ionic diffusion/migration would depend on the film thickness, both decreasing with the latter. At the same time, the film is subjected to a chemical dissolution in solution, the rate of which is independent of film thickness.

The rate of film growth may, therefore, be approximated as

$$\frac{dL}{dt} = A' I_{corr} - v_c = \frac{A}{L} - v_c \tag{11}$$

where A is a constant dependent on the film properties such as its conductivity, concentration of diffusing species etc. and v_c is the rate of chemical dissolution of the film.

Equation (11) on integration gives:

$$\frac{1}{v_c^2}\left[A\left\{\ln\left(\frac{A - v_c L_0}{A - v_c L}\right)\right\}\right] - v_c(L - L_0) = t \tag{12}$$

where L_0 is the film thickness at $t = 0$. This represents an exponential growth for the film as observed experimentally.

A plot of the rate of film growth, obtained from a differentiation of film thickness vs ageing time curves (Fig. 7), against the film thickness (Fig. 8) would give the rate constant for the film growth process. Also, the absicissa in the above linear plot yields the steady-state film thickness from which could be calculated the rate of chemical dissolution of the film. The rate constants thus calculated for uncoated and chromate-passivated Mg are $3.33 \times 10^{-19}\,cm^2\,sec^{-1}$ and $0.434 \times 10^{-19}\,cm^2\,sec^{-1}$ respectively, the steady-state film thicknesses are 40.0 and 9.5 Å and the film dissolution

* The film thicknesses calculated above should only be regarded as *relative* in view of the several assumptions involved in their calculation. For example the roughness factor could be much higher than unity for an etched and hence rough electrode; the dielectric constant could be much higher for the wet and hydrated film than for the bulk sample of film material. As such, the above film thicknesses may be lower than true values. Moreover, these measurements are not accurate in solutions without chromate wherein the anode film is unstable and dissolves rapidly. The dielectric constants of $Mg(OH)_2$, $MgCrO_4$ are assumed to be 8.2, since the dielectric constants of Mg compounds, for e.g., MgO, $MgSO_4$ and $MgCO_3$ are 8.2, 8.2 and 8.1 respectively. The dielectric constants of coconut oil and olive oil are around 3.0 [15].

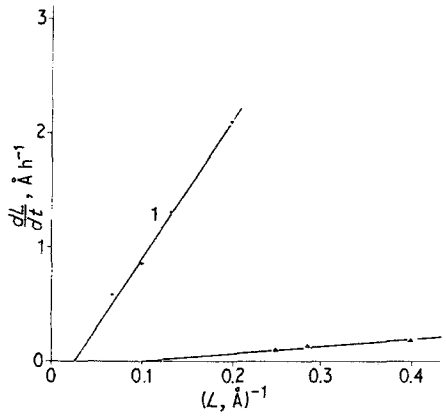

Fig. 8. Dependence of net rate of film growth, dL/dt on the reciprocal film thickness $1/L$ over (1) uncoated and (2) chromate-passivated Mg anode during its ageing in 1 N $Mg(ClO_4)_2$ solution saturated with $Mg(OH)_2$ (pH: 8.5) and containing 0.3 g l^{-1} of Li_2CrO_4.

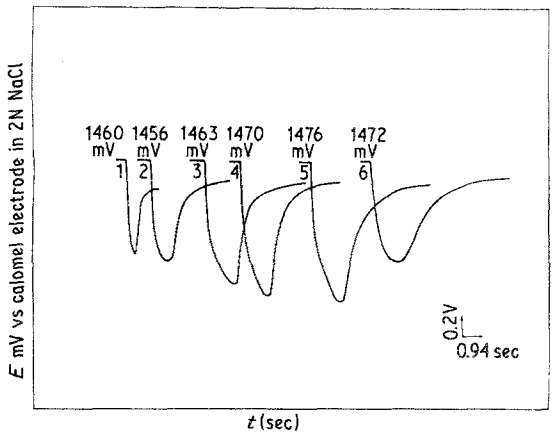

Fig. 9. Delay-time curves of uncoated Mg anode at a c.d. of 1 mA cm^{-2} after ageing for (1) 15 min; (2) 6 h; (3) 23 h; (4) 47 h; (5) 54 h and (6) 147 h, in 1 N $Mg(ClO_4)_2$ solution saturated with $Mg(OH)_2$ (pH: 8.5).

rates are 8.325×10^{-13} and 4.55×10^{-13} cm s^{-1} respectively.

It is thus clear that the kinetic constant for film growth decreases on chromate passivation owing to a reduced corrosion of Mg. As a result, the steady-state film thickness is lower on chromate passivated Mg as compared to uncoated Mg, despite a lower film dissolution rate in the former. It therefore follows that $MgCrO_4$ film is more protective and tenacious than $Mg(OH)_2$ film.

Similar calculations were not made for oil-coated Mg since the mechanisms of ionic conduction are not applicable in this case.

4.4. *Solutions without chromate*

4.4.1. Uncoated Mg. The transient behaviour on galvanostatic micropolarization of uncoated Mg disappears within 18 h of ageing of the anode in solutions without chromate. The interfacial resistance thus becomes unnoticeably low pointing to a dissolution of the initial anode film during ageing. Accordingly, the uncoated Mg is expected to exhibit shorter voltage delay during its ageing. The delay transient, on the other hand, was found to be increasing with an increase in the potential dip as well as time of potential recovery [Fig. 9; also see Fig. 4 in [1]] which may be explained as below.

One of the important factors affecting the growth of the passive film is the mechanism of precipitation of corrosion products. In cases where a larger part of them precipitates directly on the anode surface to form a compact barrier-type layer, there would be an increase in the interfacial resistance as measured from potential transients during micropolarization. In a situation where the corrosion products diffuse into the solution and precipitate away from the anode surface to form a secondary porous layer, there would be no increase in the film resistance and no growth in the anode film as estimated from potential transients under study. Instead, the initial passive film becomes thinner during ageing due to its chemical dissolution in the solution.

In solutions containing chromate, the corrosion products especially $MgCrO_4$, deposit readily on the anode surface forming a compact barrier-type layer over the initial passive film. This is aided by the fact that $MgCrO_4$ sediments at a pH lower than that of the solution under study. Also, $MgCrO_4$ precipitate is highly crystalline which would help form a coherent deposit. In solutions devoid of chromate, on the other hand, the corrosion products, mainly $Mg(OH)_2$, would not deposit as readily. Nor do they diffuse far away from the electrode into the bulk of the solution and dissolve in the latter, since the solution is presaturated with $Mg(OH)_2$. Consequently, the corrosion products settle down near the electrode forming a secondary porous layer which grows at a faster rate on ageing due to a higher corrosion rate of Mg (Table 1). The above model is consistent also with the well-known slow dissolution/precipitation kinetics as well as highly non-crystalline amorphous or colloidal nature of $Mg(OH)_2$.

4.4.1.1. Surface film observations by scanning electron microscopy (SEM). The surfaces of Mg anodes aged for 3 days in solutions with and without chromate inhibitor have been examined by SEM at different magnifications. The microstructures (Fig. 10) conform to the above deductions on the film morphology made from the potential transients at low c.d.s and delay time curves during ageing.

The deposit of corrosion products over Mg anode aged in solutions containing chromate appears crystalline, coherent and nonporous (Fig. 10a), whereas in solutions without chromate inhibitor the anode film shows several discontinuities such as fissures/deep cracks etc. (Fig. 10b).

4.4.1.2. Voltage delay of porous film. The bulky porous layer of $Mg(OH)_2$ would neither possess any protective properties nor would it exhibit potential transient during micropolarization. Nevertheless, the porous film contributes to a substantial voltage delay due to diffusion polarization at the interface as also observed with Li anodes [16]. The porous layer can be

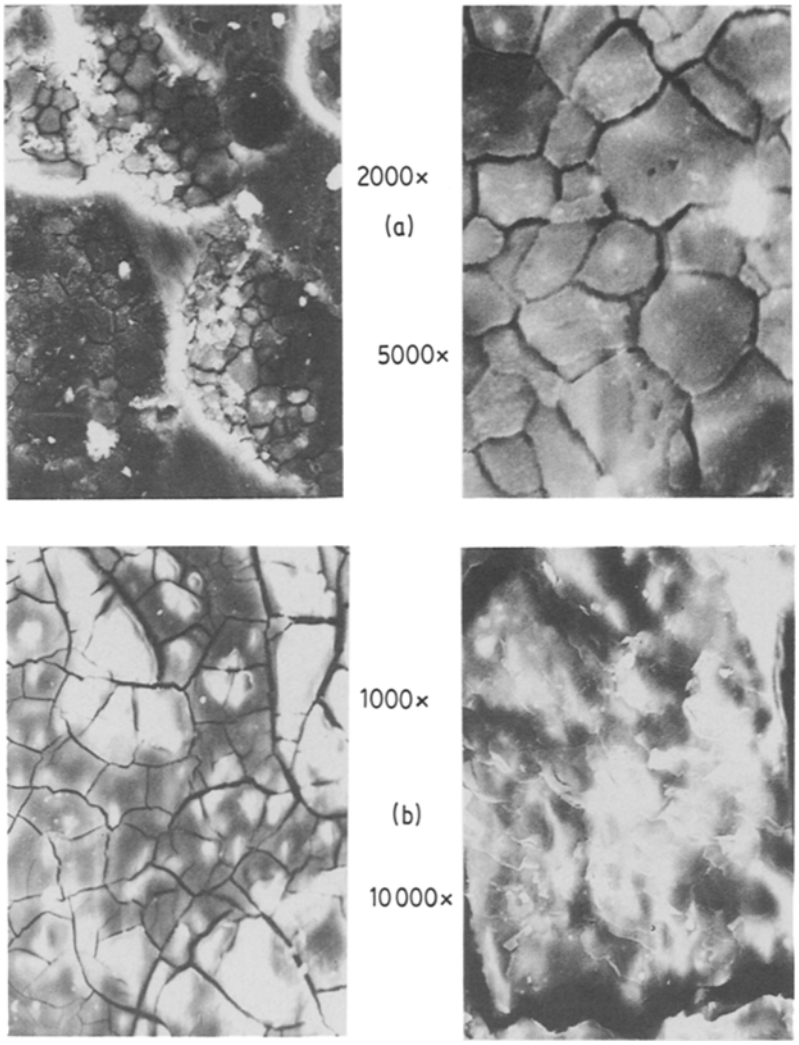

Fig. 10. SEM pictures of uncoated Mg anode aged for 3 days in 1 N $Mg(ClO_4)_2$ solution saturated with $Mg(OH)_2$ (pH: 8.5) (a) with, and (b) without 0.3 g l^{-1} of Li_2CrO_4.

looked upon as a membrane which slows down the transport of ions across it. In particular, the diffusion of $Mg(OH)_2$ is greatly hindered due to presaturation of the bulk solution with the same. A concentration gradient of $Mg(OH)_2$ thus sets in within the pores: its accumulation would build up a high resistance across film resulting in an increasing anodic polarization. Further dissolution of Mg generates sufficient dilatation stress in the film, due to bulky $Mg(OH)_2$, as to cause a mechanical rupture of the film and thus a recovery in the electrode potential as proposed in [1].

The delay time transients in solutions without chromate exhibit several features associated with diffusion limited processes such as absence of instantaneous potential (*IR*) drop and a slow approach to and, also slow recovery from the potential dip, resulting in a long voltage delay. The delay time profiles are typically broad and u-shaped as compared to the sharp v-shaped transients in solutions containing chromate. Further, the plot of electrode potential against $t^{-1/2}$ (Fig. 11) is linear (the intercept on the η axis being the *IR* drop across the porous film at t_∞ after current injection) thus confirming that the anodic polarization is essentially due to slow diffusion processes.

It may therefore be concluded that a compact, barrier-type film builds up over initially passive Mg during ageing in solutions containing chromate. In solutions without chromate, on the other hand, a bulky porous film grows, after a dissolution of initial passive film, which contributes to a long voltage delay by 'diffusion polarization'. It is thus advisable to add chromate to the electrolyte not only to inhibit the corrosion of Mg, but also to control the 'morphology' of the film suitably for a short voltage delay.

4.4.2. Coated Mg. The potential-time transients during micropolarization of coated Mg also diminish in size during ageing in solutions without chromate. The transient behaviour is totally absent after 18 h of ageing of chromate-passivated Mg, whereas with oil-coated Mg the decrease in the transient behaviour is not as rapid. In all cases, there is a continuous decrease in the film resistance and increase in film capacitance as a result of rapid dissolution of anode film (Fig. 12). As mentioned above, there is no growth of barrier-type anode film to compensate for its chemical dissolution in solutions without chromate resulting in a net film dissolution.

The tenacity in anodic coatings increases as

$$\text{magnesium hydroxide} < \text{magnesium chromate} \ll \text{coconut oil or olive oil}$$

The tenacity of oil coating as compared to chromate

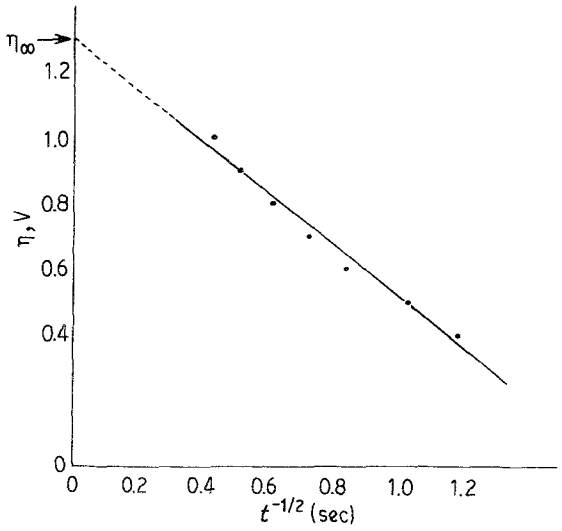

Fig. 11. Linear dependence of overpotential on $t^{-1/2}$ during voltage delay at 1 mA cm^{-2} of uncoated Mg anode in contact with 1 N $Mg(ClO_4)_2$ solution saturated with $Mg(OH)_2$ (pH: 8.5), recast from curve 6 in Fig. 9.

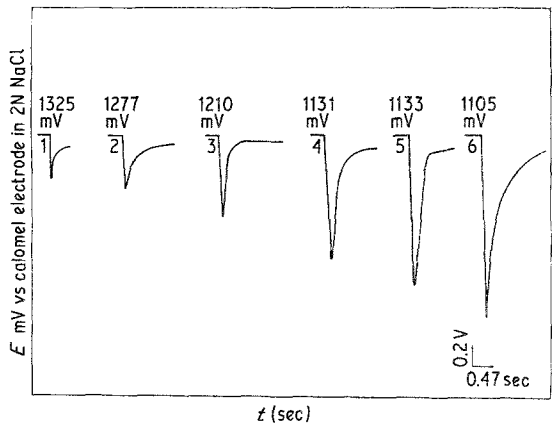

Fig. 13. Delay time curves of chromate-passivated Mg anode in contact with 1 N $Mg(ClO_4)_2$ solution saturated with $Mg(OH)_2$ (pH: 8.5) and containing 0.3 g l^{-1} of Li_2CrO_4 at a c.d. of 1 mA cm^{-2} and at a temperature of (1) 27° C; (2) 10° C; (3) 0° C; (4) −10° C; (5) −20° C and (6) −27° C.

passivation could be due to the hydrophobicity of oils resisting the breakdown/dissolution of the film by H^+, ClO_4^- ions. Olive oil coating is more tenacious than coconut oil coating, as may be expected from a lower dissolution rate of olive oil in alkaline solutions.

The longevity of the passive film, its dissolution kinetics during ageing of the anode in solution, and hence, the corrosion resistance of Mg anode in Mg batteries, could thus be evaluated from the film resistance/capacitance measurements using the above d.c. micropolarization technique.

4.5. *Transients at low temperatures*

The voltage delay of Mg anode and hence of Mg batteries increases sharply with a decrease in the ambient temperature as is illustrated by the family of delay time curves (Fig. 13) of the chromate-passivated Mg in chromate-containing solution. There is an increase in the potential dip with a decrease in temperature pointing out a rise in the interfacial resistance at low temperatures.

The potential-time transients during micropolarization of Mg for example of chromate-passivated Mg in chromate-containing solutions (Fig. 14) also increase with a decrease in temperature. (Chromate-passivated Mg in solutions containing chromate aged for about 16 h has been chosen for this study in order to have minimum changes in the film thickness during the above measurements at different temperatures, which is confirmed by an absence of decrease in the film capacitance (with dielectric constant not varying much with temperature in this case). The oil-coated anodes are not suitable since the mechanisms of ionic migration/diffusion are inapplicable.) The film resistance measured therefrom increases exponentially (Fig. 15) with a decrease in temperature. The film capacitance, on the other hand, remains the same with no noticeable decrease (Fig. 15) implying that no film growth occurred during the above measurements. It may, therefore, be inferred that the resistivity of the film material goes up at low temperatures.

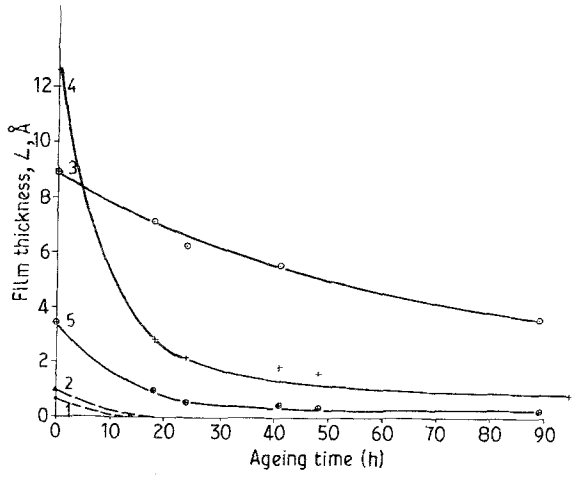

Fig. 12. Decrease of film thickness over (1) uncoated, (2) chromate-passivated, (3) olive oil-coated, (4) coconut oil-coated and (5) chromate-passivated and coconut oil-coated Mg anode during its ageing in 1 N $Mg(ClO_4)_2$ solution saturated with $Mg(OH)_2$ (pH: 8.5).

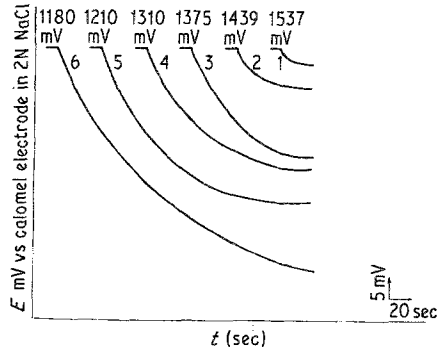

Fig. 14. Potential-time transients of chromate-passivated Mg anode (area: 5 cm^2) in contact with 1 N $Mg(ClO_4)_2$ solution saturated with $Mg(OH)_2$ (pH: 8.5) and containing 0.3 g l^{-1} of Li_2CrO_4 during micropolarization of 20 nA cm^{-2} and at a temperature of (1) 27° C; (2) 10° C; (3) 0° C; (4) −10° C; (5) −20° C and (6) −27° C.

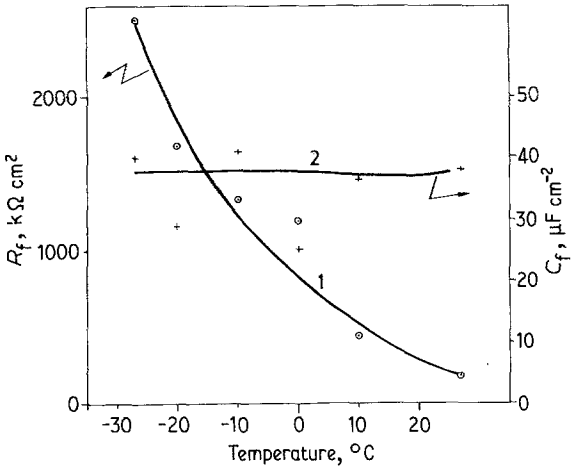

Fig. 15. Temperature dependence of (1) resistance and (2) capacitance of passive film over chromate-passivated Mg in contact with 1 N $Mg(ClO_4)_2$ solution saturated with $Mg(OH)_2$ (pH: 8.5) and containing 0.3 g l^{-1} of Li_2CrO_4.

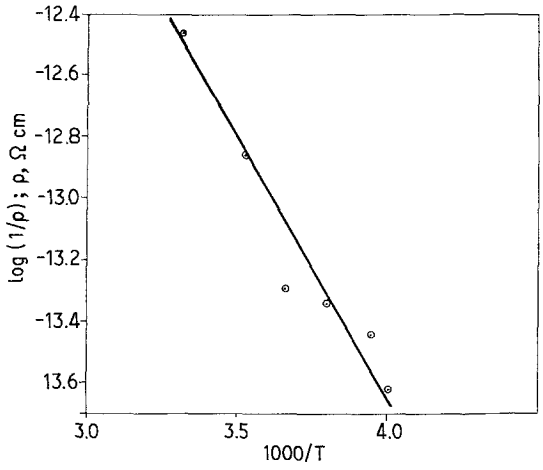

Fig. 16.Temperature dependence of the ionic conductivity through the film over chromate-passivated Mg in contact with 1 N $Mg(ClO_4)_2$ solution saturated with $Mg(OH)_2$ (pH: 8.5) and containing 0.3 g l^{-1} of Li_2CrO_4.

From the temperature dependence of the resistivity of the passive film, the apparent activation energy of the ionic conductivity could be assessed. The Arrhenius plot of ln $(1/\varrho)$ vs 1/T (Fig. 16) yields a value of 0.2065 e.v. as the activation energy for the film material, i.e. essentially $Mg(OH)_2$ and $MgCrO_4$.

5. Conclusions and other applications

The resistance and capacitance of passive films on Mg anodes in contact with electrolyte could be determined from transient and steady-state response of the electrode potential to low amplitude galvanostatic polarization, non-destructively and also in a simple manner as compared to the methods adopted hitherto.

The resistances and capacitances of the anode films are typically of the order of 10^4–$10^5\,\Omega\,cm^2$ and 10^{-6}–$10^{-5}\,F\,cm^{-2}$ respectively. Oil-coated Mg anodes exhibit higher interfacial resistance, lower capacitance and hence a lower corrosion rate.

From the potential transients at various intervals during ageing of the anode in solution, it is possible to follow the growth/dissolution kinetics of the anode film. In solutions containing chromate inhibitor, the anode film builds up at a rate proportional to the corrosion rate of the anode. In solutions without chromate, there is a progressive dissolution of the film due to attack by ClO_4^-, H^+ ions, oil coating being more tenacious than either $Mg(OH)_2$ or $MgCrO_4$ film. At low temperatures, the film resistivity rises exponentially causing high ohmic polarization at the interface and therefore a long voltage delay.

A combination of potential transients at low and high c.d.s during ageing of the anode in solution helps to predict the morphology of the anode film. In solutions containing chromate, a barrier type film which causes voltage delay by 'ohmic polarization' builds up. In the absence of chromate in solution, on the other hand, a porous layer which contributes to voltage delay by 'diffusion polarization' deposits on the anode. These observations have been verified by scanning electron microscopy.

Finally, it may be possible to adopt this technique, i.e. a combination of potential transients at low as well as high c.d. during ageing of the anode in solution, in secondary lithium batteries to identify the suitable electrolyte/solvent system for a high cycling efficiency.

To alleviate passivation-related problems of secondary Li anodes, it is essential to have anode films, if any, of suitable type, e.g. in 2Me-THF/$LiAsF_6$, which is favourable to 'recontacting of Li' – a manifestation of a porous film and/or an electronically conductive [17–19] film, both of which could be characterized *in situ* and also in a simple and rapid manner by the above technique.

Acknowledgements

The author is grateful to Professor S. Sathyanarayana, Indian Institute of Science, Bangalore, India for many useful discussions and helpful suggestions and to Dr G. Manohar, Deputy General Manager, Battery Division, Bharat Electronics Ltd., Pashan, Pune for his keen interest and encouragement and to M/s Bharat Electronics Ltd., Pune, India for providing the facilities during the period of this work. This work was also supported, in part, by the National Aeronautics and Space Administration at the Jet Propulsion Laboratory, California Institute of Technology. The author acknowledges the support of the National Research Council Resident Associate Program at Jet Propulsion Laboratory.

References

[1] B. V. Ratnakumar and S. Sathyanarayana, *J. Power Sources* **10** (1983) 219.
[2] S. Sathyanarayana and B. V. Ratnakumar, *ibid.* **10** (1983) 243.
[3] D. V. Kakoulina and B. N. Kabanov, *Zh. Fiz. Khim.* **34** (1960) 2469; *Russ. J. Phys. Chem.* **31** (1960) 1165.
[4] M. L. Gopikanth and S. Sathyanarayana, *J. Appl. Electrochem.* **9** (1979) 581.

[5] G. R. Hoey and M. Cohen, *J. Electrochem. Soc.* **106** (1959) 776.
[6] G. G. Perrault, *J. Electroanal Chem.* **27** (1970) 47.
[7] *Idem*, 'Encyclopaedia of Electrochemistry of Elements', Vol. VIII, Ch. 4, edited by A. J. Bard, Marcel Dekker, NY,(1978).
[8] R. V. Moshtev, Y. Geronov, B. Puresheva and A. Nassalevska, Extended Abstracts, No. 153, 28th ISE Meeting, (Varna, 1977).
[9] R. V. Moshtev, Y. Geronov and B. Puresheva, *J. Electrochem. Soc.* **128** (1981) 1851.
[10] Y. Geronov, F. Schwager and R. H. Muller, *ibid.* **129** (1982) 1422.
[11] R. V. Moshtev and Y. Geronov, *J. Power Sources* **8** (1982) 395.
[12] Y. Geronov, R. V. Moshtev and B. Puresheva, Proc. Int. Meeting on Li Batteries, Rome (1982).
[13] S. R. Narayanan and S. Sathyanarayana, *J. Power Sources* **15** (1985) 27.
[14] B. V. Ratnakumar and S. Sathyanarayana, *ibid.* **12** (1984) 39.
[15] D. Dobos, in 'Electrochemical Data', Elsevier Scientific Publishing Co. (1975).
[16] E. Peled, 'Lithium Batteries', Ch. 3, edited by J. P. Gabano, Academic Press (1983) p. 59.
[17] S. B. Brummer, Proc. of Workshop on Li Non-aqueous Battery Electrochem., Publication 80-7, The Electro-',chem. Soc., N.J. (1980).
[18] S. B. Burmmer, V. R. Koch and R. D. Rauh, 'Materials for Advanced Batteries', edited by D. W. Murphy, J. Broadhead and B. C. H. Steele, Plenum Press, New York (1980) p. 123.
[19] K. M. Abraham and S. B. Brummer, 'Lithium Batteries', edited by Jean Paul Gabano, Academic Press (1983).